Initial state-selected reaction probabilities for $OH+H_2 \rightarrow H+H_2O$ and photodetachment intensities for HOH_2^-

Ward H. Thompson and William H. Miller
Department of Chemistry, University of California, and Chemical Sciences Division, Lawrence Berkeley Laboratory, Berkeley, California 94720

(Received 14 June 1994; accepted 2 August 1994)

We have used a discrete variable representation (DVR) with absorbing boundary conditions (ABC) to calculate initial state-selected reaction probabilities and photodetachment intensities. We apply this method to the $OH+H_2$ reaction constrained to a plane with the OH bond frozen. The calculated reaction probabilities have all the qualitative features observed in full dimensional calculations. We have similarly computed arrangement-selected photodetachment intensities for one geometry of the HOH_2^- anion. The resulting spectrum has a dominant peak which will present a test of the neutral potential energy surface upon comparison with experimental results.

I. INTRODUCTION

Quantum mechanical scattering calculations have advanced to the point that rigorous calculations are now possible for a number of atom–diatom reactions[1] ($A+BC \rightarrow AB+C$), and the first attempts at rigorous treatments of four atom reactions are beginning to appear.[2–11] Due to the light masses involved and the availability of a reasonable potential energy surface, the

$$OH+H_2 \rightarrow H_2O+H \tag{1.1}$$

reaction has become the benchmark of choice for exact quantum treatments of a diatom–diatom collision. Already, there have been two full dimensional state-selected time-dependent wave packet calculations[9,10] on this system as well as a time-independent calculation of the cumulative reaction probability using a discrete variable representation (DVR) with absorbing boundary conditions (ABC) to represent the Green's function.[11]

Despite the advances of the last decade, exact quantum scattering calculations remain unfeasible for systems with five or more atoms and indeed, for most four atom reactions. At the same time, it may not be necessary to treat all the degrees of freedom in a large system using rigorous quantum mechanics. An excellent example of this is the OH bond in reaction (1.1). *Ab initio* calculations show that the bond distance hardly changes throughout the entire reaction,[12] and the full dimensional dynamics calculations show that freezing this bond has a minimal effect on the reaction probabilities.[9,10] The logical approach to treating a large system "rigorously" may lie in reduced dimensionality, mixed quantum-classical,[13,14] or mixed quantum-semiclassical approaches.[15]

Numerous reduced dimensionality studies have been performed on reaction (1.1) and its isotopic variants. Clary and co-workers[2–4] have calculated state-to-state S-matrix elements using the rotating bond approximation (RBA) and obtained good agreement with experimental results.[4] Echave and Clary have also carried out a full planar calculation.[5] Wang and Bowman have used the adiabatic bend approximation to compute state-to-state probabilities and cross sections.[6] Their results show mode-specificity for the $H+H_2O$ reaction in agreement with the experimental results of Crim[16] and Zare.[17] Baer and co-workers have treated the reaction using a sudden approximation for the angular degrees of freedom.[7]

Comparison of reactive scattering calculations and experiments can provide a great deal of information about the potential energy surface. However, many details are obscured by summing over all the partial waves.[18] In addition, the results depend not only on the transition state region, but also on the features of the entrance and exit channels. Neumark and co-workers[19] have been able to access information about the transition state directly by performing photodetachment experiments. Comparison with theoretical calculations can give detailed information about the transition state, as has been seen for the $F+H_2$ reaction.[20,21]

The DVR-ABC formalism for calculating the full reactive scattering Green's function was first introduced by Seideman and Miller[22] and applied to cumulative reaction probabilities. Subsequently it was shown to be an efficient method for calculating *state-specific* reaction probabilities.[23,24] The purpose of this paper is twofold: (1) to test the DVR-ABC method on a large multidimensional reactive scattering system, and (2) to show how the same formalism can be used to efficiently calculate photodetachment intensities.

In Sec. II we outline the DVR-ABC formalism for calculating initial state-selected reaction probabilities and photodetachment intensities. We also show how this method allows us to obtain arrangement-selected intensities with no increase in computational effort. Section III discusses the details of the calculations including the Hamiltonian, the basis set, the asymptotic state, and the iterative methods used to solve the linear algebra problem. Section IV presents the results of the scattering and photodetachment calculations, and Sec. V concludes.

II. SUMMARY OF THEORY

Here, we outline the basic DVR-ABC formulas used in this study to calculate both initial state-selected probabilities and photodetachment intensities. Before embarking on this, we note that the discrete variable representation, and other

 0021-9606/94/101(10)/8620/8/$6.00

grid point methods, has been developed and used by many persons,[25–35] with the work of Light *et al.*[36] being particularly important in recent years. Also, an absorbing potential (negative imaginary potential, optical potential) has been used by a number of workers in both time-dependent[37–40] and time-independent[41–43] frameworks. By the "DVR-ABC approach" summarized below we mean the specific representation of the outgoing wave Green's function using these techniques and the scattering formulae that result from it.

A. Reactive scattering

The DVR-ABC approach has been demonstrated to be an efficient method for calculating cumulative,[11,22] initial state-selected,[23,24] and state-to-state reaction probabilities.[23] The methodology has been described in detail elsewhere;[23] here we will provide a brief summary.

In this paper we are interested only in the total reaction probability from a given state of the reactants. This probability is defined in terms of the state-to-state S-matrix elements as

$$P_{\mathbf{n}_r}(E) \equiv \sum_{\mathbf{n}_p} |S_{\mathbf{n}_p,\mathbf{n}_r}(E)|^2. \tag{2.1}$$

where $\mathbf{n}_r$ and $\mathbf{n}_p$ represent the set of reactant and product quantum numbers, respectively. In the DVR-ABC formalism, all of the computational effort is placed in computing the scattering Green's function with outgoing wave boundary conditions,

$$\hat{G}^+(E) = (E - \hat{H} + i\epsilon)^{-1}. \tag{2.2}$$

This is accomplished by allowing the "$i\epsilon$," which is added to the energy to enforce the outgoing wave boundary conditions, to be a function of position. That is, $\epsilon(\mathbf{q})$ is zero in the interaction region and "turns on" in the reactant and product valleys. These absorbing boundary conditions allow the use of a basis which is localized in the interaction region to represent the Green's function.

For the purpose of general use in large dimensional problems, we have chosen to use a DVR basis (see Sec. III A). The initial state-selected reaction probability is then given by

$$P_{\mathbf{n}_r}(E) = \frac{2}{\hbar} \boldsymbol{\Psi}^{T*}_{\mathbf{n}_r} \cdot \boldsymbol{\epsilon}_p \cdot \boldsymbol{\Psi}_{\mathbf{n}_r}, \tag{2.3}$$

where all bold face quantities are vectors or matrices in the DVR, and $\boldsymbol{\epsilon}_p(\boldsymbol{\epsilon}_r)$ is the part of the absorbing potential in the product (reactant) arrangement. $\boldsymbol{\Psi}_{\mathbf{n}_r}$ is the reactive scattering wave function for an initial state $\mathbf{n}_r$ of the reactants. This is obtained from the asymptotic state of the reactants $\boldsymbol{\Phi}_{\mathbf{n}_r}$ by the DVR-ABC version of the Lippmann–Schwinger equation

$$\boldsymbol{\Psi}_{\mathbf{n}_r} = i\mathbf{G}^+(E) \cdot \boldsymbol{\epsilon}_r \cdot \boldsymbol{\Phi}_{\mathbf{n}_r}. \tag{2.4}$$

As has been noted previously,[23] this formulation for obtaining the initial state-selected probability has the advantage of requiring less computational effort than a corresponding calculation of the more detailed state-to-state probabilities.

B. Photodetachment intensity

The photodetachment intensity is given within the Franck–Condon approximation by

$$I(E) = \sum_{\mathbf{n}_\gamma = \mathbf{n}_r, \mathbf{n}_p} \rho(E) |\langle \Psi_{\mathbf{n}_\gamma}(E) | \phi_b \rangle|^2, \tag{2.5}$$

where ϕ_b is the bound state of the anion. The density of states, $\rho(E)$, is associated with the normalization of the scattering wave function, which for our choice of normalization is $\rho(E) = (2\pi\hbar)^{-1}$. This approximation has been shown to be very useful and accurate.[21,44]

In the DVR-ABC approach Eq. (2.4) is used to obtain the reactive scattering wave function. The bound state DVR vector can be obtained by solving an eigenvalue problem using the same basis as for the scattering wave function. The Franck–Condon intensity is thus given by

$$I(E) = \frac{1}{2\pi\hbar} \sum_{\mathbf{n}_\gamma = \mathbf{n}_r, \mathbf{n}_p} \boldsymbol{\phi}_b^\dagger \cdot \mathbf{G}^*(E) \cdot \boldsymbol{\epsilon}_\gamma \cdot \boldsymbol{\Phi}^\dagger_{\mathbf{n}_\gamma} \boldsymbol{\Phi}_{\mathbf{n}_\gamma} \cdot \boldsymbol{\epsilon}_\gamma \cdot \mathbf{G}(E) \cdot \boldsymbol{\phi}_b. \tag{2.6}$$

However, one can make use of the closure relation derived in Ref. 23 to obtain the following simpler result:

$$I(E) = \frac{1}{\pi} \boldsymbol{\phi}_b^\dagger \cdot \mathbf{G}^*(E) \cdot \boldsymbol{\epsilon} \cdot \mathbf{G}(E) \cdot \boldsymbol{\phi}_b, \tag{2.7}$$

for the total photodetachment intensity. Moreover, since the full absorbing potential can be written as the sum of the absorbing potentials in the reactant and product arrangements, $\boldsymbol{\epsilon} = \boldsymbol{\epsilon}_r + \boldsymbol{\epsilon}_p$, one can divide the intensity into the parts due to the neutral dissociating into reactants and the part dissociating into products (that is, *arrangement-selected* intensities). Then the contribution from a given arrangement γ is given by

$$I_\gamma(E) = \frac{1}{\pi} \boldsymbol{\phi}_b^\dagger \cdot \mathbf{G}^*(E) \cdot \boldsymbol{\epsilon}_\gamma \cdot \mathbf{G}(E) \cdot \boldsymbol{\phi}_b. \tag{2.8}$$

Alternatively, starting again from Eq. (2.5), we can use the completeness relation for the scattering wave function

$$\sum_{\mathbf{n} = \mathbf{n}_r, \mathbf{n}_p} \rho(E) |\Psi_{\mathbf{n}}(E)\rangle\langle\Psi_{\mathbf{n}}(E)| = \delta(E - \hat{H}). \tag{2.9}$$

The right-hand side is just the microcanonical density operator which can be expressed in terms of the outgoing wave Green's function

$$\delta(E - \hat{H}) = -\frac{1}{\pi} \operatorname{Im} \hat{G}^+(E). \tag{2.10}$$

This gives us an alternative, direct way to calculate the total photodetachment intensity. In the DVR-ABC formulation this is given by

$$I(E) = -\frac{1}{\pi} \operatorname{Im} \boldsymbol{\phi}_b^\dagger \cdot \mathbf{G}^+(E) \cdot \boldsymbol{\phi}_b. \tag{2.11}$$

Note that both methods require the same amount of computational work: the action of the Green's function onto a

single vector. Thus the direct and arrangement-selected photodetachment intensities can be computed by Eqs. (2.11) and (2.8) simultaneously with no extra work.

III. DETAILS OF CALCULATION

A. The Hamiltonian and the basis set

Since we are interested in initial state-selected quantities, we have chosen to use the Jacobi coordinates of the reactants. This coordinate system is advantageous for describing the asymptotic states of the reactants. We denote the H_2 and OH bond distances by R_1 and R_2, respectively. The distance between the H_2 and OH centers of mass is R_3. γ_1 is the angle between $\mathbf{R}_1$ and $\mathbf{R}_3$, γ_2 the angle between $\mathbf{R}_2$ and $\mathbf{R}_3$, and φ is the torsional angle.

We have calculated reaction probabilities and photodetachment intensities explicitly treating four degrees of freedom. The OH bond distance is frozen at its equilibrium value and the torsional angle is fixed at $\varphi=0$, i.e., the planar configuration. These give the proper transition state geometry for the reaction. The quality of these approximations can be seen in comparing our results to the higher dimensional reactive scattering calculations. One can obtain the reduced dimensionality Hamiltonian in a straightforward way from the full Hamiltonian. The four degree-of-freedom Hamiltonian for $J=0$ is given by

$$\hat{H}=-\frac{\hbar^2}{2\mu_1}\frac{\partial^2}{\partial R_1^2}-\frac{\hbar^2}{2\mu_3}\frac{\partial^2}{\partial R_3^2}+\left(\frac{1}{2\mu_1 R_1^2}+\frac{1}{2\mu_3 R_3^2}\right)\hat{\mathbf{j}}_1^2+\left(\frac{1}{2\mu_2 R_2^2}+\frac{1}{2\mu_3 R_3^2}\right)\hat{\mathbf{j}}_2^2+\hat{V}(R_1,R_2=R_2^{\mathrm{eq}},R_3,\theta_1,\theta_2,\varphi=0), \tag{3.1}$$

where $\hat{\mathbf{j}}_1$ and $\hat{\mathbf{j}}_2$ are the angular momentum operators for the H_2 and OH rotation, respectively. We will use j_1 and j_{H_2} interchangeably for the H_2 rotation quantum number and similarly j_2 and j_{OH}.

In our calculations we have used the potential energy surface fit by Schatz and Elgersma[45] to the *ab initio* results of Walch and Dunning[12] (the WDSE surface). This surface also includes a modification by Clary[2] to remove a spurious well on the OH+H_2 side of the barrier.

The basic formalism outlined in Sec. II could equally well be applied using a finite basis representation other than a DVR. However, the DVR basis has the advantages that the potential energy is a diagonal matrix and the Hamiltonian matrix is sparse for a multidimensional problem. The former means that no integrals need to be evaluated numerically to obtain the matrix elements of the potential. The sparsity allows the linear algebra to be solved using iterative methods (See Sec. III C) which makes large dimensional problems tractable when one cannot store the entire Hamiltonian matrix.

We have used the sinc function DVR of Colbert and Miller[35] for the R_1 and R_3 coordinates since they represent the large-amplitude motions making up the reaction coordinate. A Gauss–Legendre DVR was used for the angles γ_1 and γ_2. However, the exchange symmetry of H_2 was exploited so that, for a given parity, only half the angular DVR points were needed for γ_1. In practice, a direct product (raw) grid is first laid down in these coordinates. The "refined" grid is then obtained by truncating the raw grid according to two criterion: (1) an energy cutoff, i.e., if the potential at a given DVR point is greater than some value V_{cut}, then that point is discarded, and (2) the boundaries of the absorbing potential in the reactant and product valleys. Then the matrix elements of the Hamiltonian are computed in the DVR. Finally, the linear system

$$(E\mathbf{I}-\mathbf{H}+i\boldsymbol{\epsilon})\cdot\boldsymbol{\Psi}_{\mathbf{n}_r}=i\boldsymbol{\epsilon}_{\mathbf{r}}\cdot\boldsymbol{\Phi}_{\mathbf{n}_r} \tag{3.2}$$

is solved to obtain the reactive scattering wave function as given by Eq. (2.4).

As pointed out above, the potential energy matrix elements are diagonal. The diagonal elements are simply the potential evaluated at the DVR grid point. The DVR matrix elements of the absorbing potential are also diagonal and similarly evaluated. The radial kinetic energy matrix elements can be expressed in closed form[35] as

$$(\hat{T}_\alpha)_{i,i'}=\frac{\hbar^2}{2\mu_\alpha\Delta R_\alpha^2}(-1)^{(i-i')}\times\begin{cases}\pi^2/3-1/2i^2, & i=i'\\ \dfrac{2}{(i-i')^2}-\dfrac{2}{(i+i')^2}, & i\neq i'\end{cases} \tag{3.3}$$

where $\alpha=1$ or 3 and ΔR_α is the grid spacing. The $1D$ kinetic energy matrix elements for the angular DVR are given by a sum over Legendre polynomials:

$$(\hat{T}_{\mathrm{ang2}})_{i,i'}=\sum_{j=0}^{N-1}\sqrt{w_i}P_j(\cos\gamma_{2i})\times j(j+1)\hbar^2\sqrt{w_{i'}}P_j(\cos\gamma_{2i'}) \tag{3.4}$$

for the OH rotation, where N is the number of angular DVR points. For the H_2 rotation, the symmetrized matrix elements are given by

$$(\hat{T}_{\mathrm{ang1}})^p_{i,i'}=\sum_{j=0}^{N-1}\sqrt{w_i}P_j(\cos\gamma_{1i})j(j+1)\hbar^2\times\frac{1}{\sqrt{2}}[1+(-1)^{(p+j)}]\sqrt{w_{i'}}P_j(\cos\gamma_{1i'}) \tag{3.5}$$

where p is the parity quantum number. Note that for the symmetrized case we use only half of the angular DVR points for γ_1.

Typically we need 14 DVR points for the γ_2 and 7 points for the symmetrized γ_1 coordinate. We note that using as few as 10 and 5 angular points reduces the accuracy only slightly and produces a significant savings in the size of the basis. The number of radial DVR points are determined by specifying a grid constant, N_B, which is the number of grid points per de Broglie wavelength. A grid constant of 2.6 gives converged results. Depending on the scattering energy, the DVR basis consists of between 20 000 to as many as 50 000 points for the highest energies.

The absorbing potential is taken to be a function of the translational Jacobi coordinate in the reactant arrangement,

$\epsilon_r = \epsilon_r(R_3)$, and the H_2 bond distance in the product arrangement $\epsilon_p = \epsilon_p(R_1)$. There are several satisfactory choices for the functional form of the absorbing potential. However, any choice must turn on slowly enough not to cause reflection, yet be strong enough to absorb all outgoing flux. We have found the quartic potential to work well,

$$\epsilon_\gamma(R_\gamma) = \lambda\left(\frac{R_\gamma - R_{0,\gamma}}{R_{\max,\gamma} - R_{0,\gamma}}\right)^4 \tag{3.6}$$

where $\gamma = p, r$ is the arrangement index and $R_p = R_1$, $R_r = R_3$. $R_{0,\gamma}$ and $R_{\max,\gamma}$ are the starting and ending points of the absorbing potential in the γ arrangement. λ is a strength parameter representing the maximum value of the absorbing potential, generally it is taken to be about 2 eV. The beginning of the absorbing strip is chosen such that the imaginary potential has significant value only where the interaction potential is small.

B. The asymptotic state

The asymptotic state of the reactants used in Eq. (2.4) can be defined by

$$\hat{H}_{\text{asym}}\Phi_{\mathbf{n}_r} = \epsilon_{\mathbf{n}_r}\Phi_{\mathbf{n}_r}, \tag{3.7}$$

where $\hat{H}_{\text{asym}}$ is the asymptotic Hamiltonian for reactants given by

$$\hat{H}_{\text{asym}} = \lim_{R_3\to\infty} \hat{H}. \tag{3.8}$$

When the OH and H_2 diatoms are far apart, the eigenvalue problem defined by Eq. (3.7) is separable and becomes four, one-dimensional eigenvalue/eigenfunction problems. However, only for the H_2 vibrational eigenfunctions do we need to carry out a numerical calculation; for the translational coordinate R_3, spherical Hankel functions of the second kind are the solutions of the radial equation (including the centrifugal potential) with the proper asymptotic boundary conditions, and the OH and H_2 rotations are free rotors with Legendre polynomial eigenfunctions. Expressing the asymptotic state in a space-fixed axis, one has

$$\begin{aligned}\langle R_1, R_3, \gamma_1, \gamma_2 | \Phi_{\mathbf{n}_r}\rangle &= \varphi_v(R_1)\frac{1}{\sqrt{v_{\mathbf{n}}}} h_l^{(2)}(k_{\mathbf{n}}R_3)\sqrt{\frac{(2l+1)}{4\pi}} \\ &\times \langle j_1 0 j_2 0 | j_1 j_2 J_{12} 0\rangle \langle J_{12} 0 l 0 | J_{12} l 0 0\rangle \\ &\times \frac{1}{\sqrt{2}}[1 + (-1)^{(p+j_1)}] P_{j_1}(\cos\gamma_1) P_{j_2}(\cos\gamma_2),\end{aligned} \tag{3.9}$$

where we have noted $J = M = K = 0$. φ_v is the asymptotic H_2 vibrational eigenstate, and we have normalized the translational function with respect to the incoming flux; $k_{\mathbf{n}}$ and $v_{\mathbf{n}}$ are the translational wave vector and velocity, respectively. The Clebsch–Gordan coefficients are derived from the body-fixed to space-fixed transformation. J_{12} is the vector addition of the diatom angular momenta, j_1 and j_2, and $J = 0$ is obtained from the vector addition of J_{12} and l. p defines the parity of the H_2 rotation, and l is the orbital angular momentum quantum number.

C. Iterative methods

For a multidimensional problem, the Hamiltonian is often too large to store in core memory. There are several suitable iterative methods one can use which require only the ability to multiply the Hamiltonian onto a vector. For the reactive scattering calculations we have used the Newton algorithm developed by Auerbach and Leforestier.[24,46] This method has the advantages that it requires very little core memory (our largest calculations use only ≈10 MB), displays rapid convergence, and gives the ability to "dial in" the allowed error.

For the photodetachment calculations, we used the generalized minimum residual (GMRES) algorithm.[47] This method requires much more core memory, however, it has better convergence properties than other iterative methods since the Krylov vectors are explicitly reorthogonalized. Thus for an $N\times N$ matrix, one is guaranteed to converge in N iterations. The reason a different method is necessary for the photodetachment calculations lies in the difference of the right-hand sides (i.e., the vectors the Green's function acts on). In this case the right-hand side is the anion bound state which has very little net momentum on the neutral surface. Any method which is based on a time-dependent propagation scheme (such as Newton) will require a long propagation time and thus GMRES is preferable despite the requirement of large amounts of core memory.

IV. RESULTS

A. Initial state-selected probabilities

We have calculated initial state-selected reaction probabilities for the $OH(j_{OH}) + H_2(v, j_{H_2})$ reaction for many sets of initial quantum numbers over a range of energies. In order to compare with full dimensional calculations, the reaction probabilities as a function of translational energy are shifted, as has been done previously by Clary.[2] The shift is equal to the difference in zero point energy between the transition state and the asymptotic reactants of the neglected degrees of freedom, namely, the OH stretch and the torsional angle. This shift is 0.031 eV.[2]

The transition state on the present potential energy surface is almost collinear, with an O–H–H angle of about 164°, and it is an "early" barrier (of 0.26 eV), consistent with the exothermic character of the reaction (Hammond's postulate). Based on Polanyi's rules,[48] this would imply that translational energy would be more effective than H_2 vibration in promoting the reaction. These predictions have in fact been borne out by experiment. Light and Matsumoto found that exciting H_2 with one quantum of vibration increases the rate by about 3 orders of magnitude, while exciting both H_2 and OH gives only a slightly larger increase.[49] Zellner and Steinert observed an increase of about two orders of magnitude when the H_2 vibration is excited.[50] However they also found that the same amount of thermalized energy increases the rate by about 5000. Glass and Chaturvedi measured the same rate increase on exciting H_2 and a factor of 1.5 upon excitation of OH.[51] Recently, the first molecular beam experiment for the D_2+OH→HOD+D reaction was performed by Alagia *et al.*[52] They measured the angular distribution and

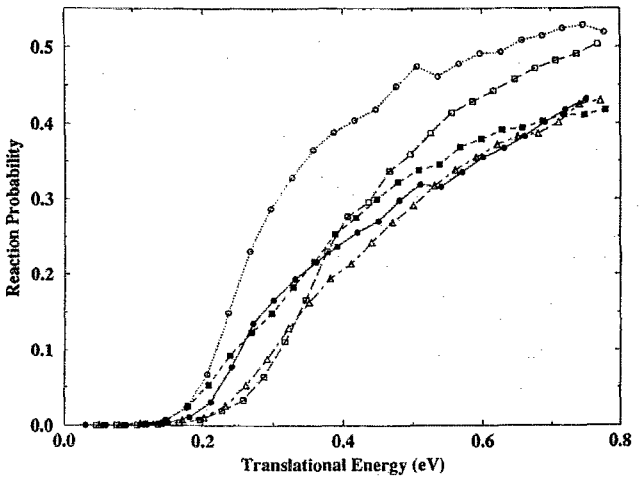

FIG. 1. Initial state-selected reaction probabilities for OH(j_{OH} = 0) + H_2(v = 0,j_{H_2}) as a function of translational energy. The reaction probability for j_{H_2} = 0 is the solid line with solid circles, j_{H_2} = 1 the dotted line with open circles, j_{H_2} = 2 the dashed line with solid squares, j_{H_2} = 3 the long dashed line with open squares, and j_{H_2} = 4 the dot–dash line with open triangles. Note these probabilities have been shifted to account for the frozen degrees of freedom (see the text).

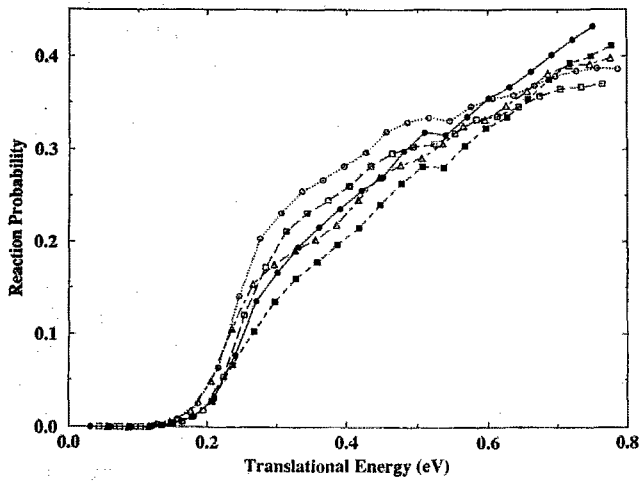

FIG. 2. Initial state-selected reaction probabilities for OH(j_{OH}) + H_2(v = 0,j_{H_2} = 0) as a function of translational energy. The symbols for the different j_{OH} are the same as for j_{H_2} in Fig. 1. These probabilities have also been shifted.

found predominantly backscattered products which is consistent with a nearly collinear transition state. Clary's three degree of freedom RBA calculations are in excellent agreement with the experimental distribution.[4]

Figure 1 shows the reaction probabilities as a function of initial j_{H_2} for v=0 and j_{OH}=0. As for the H+H_2 reaction, the probability is largest for j_{H_2} = 1. Although there is not complete quantitative agreement, the reaction probabilities shown have the same qualitative dependence on initial rotational quantum number and translational energy as the five degree of freedom results of Zhang and Zhang.[8] (We note that full dimensional calculations have shown that including the OH stretch changes the results minimally[9,10] and therefore comparing to the five degree of freedom results highlights the effect of the torsional angle.) However, our results are qualitatively different from the planar results of Echave and Clary[5] who observe a monotonic decrease in the reaction probability with initial j_{H_2}. The difference between these two planar calculations can be found in the treatment of the diatom rotations. Echave and Clary represented the diatoms as plane rotors, whereas we have treated the diatoms as three dimensional free rotors with the projection quantum number constrained to equal zero.

In Fig. 2 we show the reaction probabilities for several different values of j_{OH} with v=0 and j_{H_2} = 0. There is a very weak dependence on the initial OH rotational quantum number. This is not surprising since this rotation is not a major component of the reaction coordinate and thus should not affect the hydrogen atom transfer as strongly as the H_2 rotation. This behavior has also been observed in the planar calculations by Echave and Clary[5] as well as by Zhang and Zhang.[8,9]

The small barrier for this reaction coupled with the relatively large vibrational spacing for H_2 means that OH+H_2(v=1) proceeds virtually without a barrier. Thus the reaction probability is greatly enhanced by vibrational excitation of H_2, as noted above. Additionally, the calculations by Zhang and Zhang[9] and by Neuhauser[10] have observed strong resonance features in the reaction probabilities for initially vibrationally excited H_2. These features are also observed in our calculations as shown in Fig. 3. The lowest energy resonance is missing in our results (since we have shifted our probabilities), however, the remaining features are well reproduced.

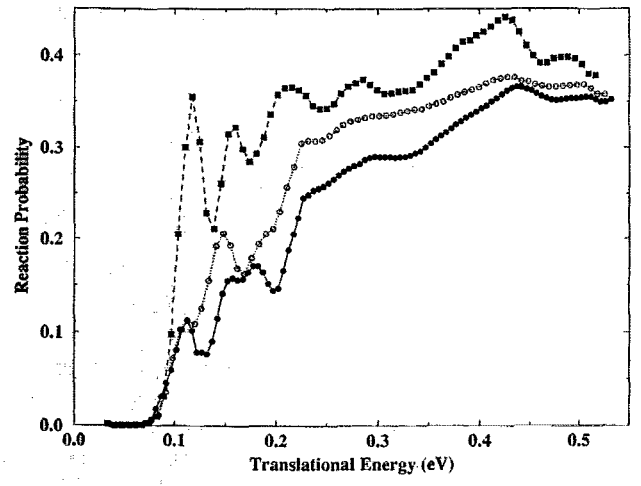

FIG. 3. Initial state-selected reaction probabilities for OH(j_{OH}) + H_2(v = 1,j_{H_2}) as a function of translational energy. The reaction probability for (j_{OH} = 0,j_{H_2} = 0) is the solid line with solid circles, (j_{OH} = 1,j_{H_2} = 0) the dotted line with open circles, and (j_{OH} = 0,j_{H_2} = 1) the dashed line with solid squares. These probabilities have also been shifted.

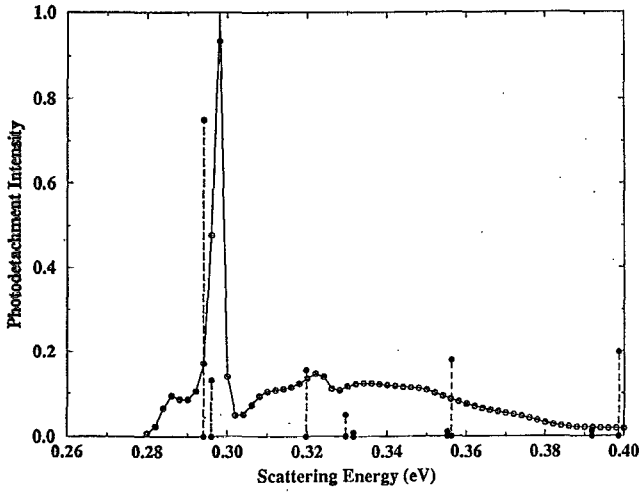

FIG. 4. Photodetachment intensities for *para* HOH_2^-. The solid line was calculated using the direct method of Eq. (2.11). The open circles were calculated by the arrangement-selected method of Eq. (2.8). The dashed lines with solid circles are the 1D Franck–Condon factors. The intensities have been scaled so that the highest point on the direct spectrum equals one. The 1D Franck–Condon factors were scaled so that the largest equals three-fourths.

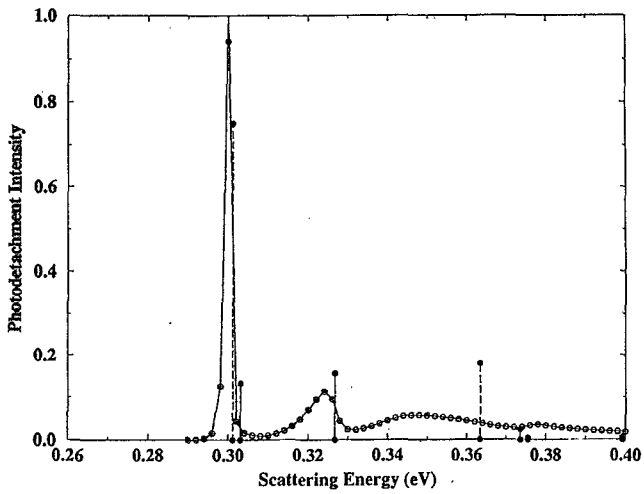

FIG. 5. Same as in Fig. 4 for *ortho* HOH_2^-.

B. Photodetachment intensities

We have also calculated intensities for photodetaching an electron from HOH_2^- to give $OH+H_2$ and $H+H_2O$. Though this system is isoelectronic with the FH_2^- system, there are many crucial differences. Xantheas and Dunning have computed critical points and force constants for the HOH_2^- anion.[53] They found two stable geometries separated by a barrier of about 2 kcal/mol. One is a linear complex of HO^- and H_2 (we will refer to this as Anion I) and the other is roughly a van der Waals complex of H_2O and H^- (Anion II). It is not clear without further *ab initio* calculations whether the anion ground state is delocalized over both geometries and if so to what degree. The Anion I geometry lies under the reactant side of the neutral surface whereas the Anion II geometry sits under the product side. Neither is close to the transition state geometry. Clearly without a relatively complete potential energy surface for the anion a delocalized ground state cannot be treated. We have chosen to address all our calculations to the Anion I geometry.

Because of the inversion symmetry of the H_2 we can carry out either *para* or *ortho* calculations. Since there is only a small barrier to internal rotation of H_2 in the anion, the *ortho* and *para* anion ground states have different energies. In terms of the neutrals formed, the *para* anion state will only give rotational states of H_2 with even parity (i.e., $j_{H_2} = 0,2,4,\cdots$) whereas the *ortho* anion state will yield only odd j_{H_2}. We have used a separable anion wave function with an equilibrium geometry defined by R_3=4.57 a.u., R_1=1.47 a.u., and $\gamma_1=\gamma_2=\pi$. We have assumed harmonic potentials with frequencies ω_3=354 cm^{-1}, ω_1=4096 cm^{-1}, $\omega_{\gamma 1}$=688 cm^{-1}, and $\omega_{\gamma 2}$=124 cm^{-1}.

Figures 4 and 5 show the photodetachment intensities using both the direct (the solid line) and arrangement-selected (the open circles) methods, Eqs. (2.11) and (2.8), respectively. The excellent agreement between these two theoretical expressions is a stringent test on the convergence of the calculation, both with respect to size of the basis and the linear algebraic calculation of the Green's function. The arrangement-selected results indicate that virtually no neutral products ($H+H_2O$) are formed and the intensity is due completely to the formation of reactants ($OH+H_2$). This is expected given the location of the anion geometry under the reactant valley of the neutral surface.

To provide qualitative insight into the spectra in Figs. 4 and 5 we consider an approximate separable model. Specifically, the scattering wave function is approximated as the product of four 1D wave functions, so that the overall Franck–Condon (FC) factor in Eq. (2.5) is the product of four 1D Franck–Condon factors. Furthermore, since the potential surface is relatively flat in the translational coordinate in the Franck–Condon region, the 1D translational wave function is taken to be a plane wave (i.e., free particle wave function). This 1D translational FC factor has an exponential peak at zero translational energy, so that the overall FC factor has a peak in the spectrum at each threshold energy that a new neutral channel opens up. Each peak has this shape of a decreasing exponential and is modulated by the product of the Franck–Condon overlaps in the three perpendicular degrees of freedom. These separable Franck–Condon factors are superimposed on the spectrum in Fig. 4.

The dominant feature in Fig. 4, a sharp peak at ~0.3 eV, is thus seen to correspond to the ground state reactant channel, $j_{H_2} = j_{OH} = 0$. Note that in this energy range we are only exciting to the ground vibrational state of H_2. The next two peaks are for $j_{H_2} = 0$ and j_{OH}=1 and j_{OH}=2. The smaller doublet around 0.33 eV corresponds to $j_{H_2} = 1$ with j_{OH}=0 and j_{OH}=1. Clearly there is significant coupling between these degrees of freedom on the neutral surface, however, this simple model allows us some insight into the origin of the prominent features of the spectrum. We should note that in reality one might see features in the spectrum due to the

torsional angle which we have frozen. However, since both the anion and neutral equilibrium geometries are planar, we would not expect this to be an important omission.

The *ortho* HOH_2^- photodetachment intensity is shown in Fig. 5 with the separable Franck–Condon factors. The 1D H_2 potential on the neutral surface also has a small barrier to rotation thereby splitting the *para* and *ortho* ground state energies. This is observed in the shift of the dominant peak to higher energies in Fig. 5. The assignment of the peaks in this case is much the same as for the *para* spectrum except that now the $j_{H_2} = 1$ doublet occurs at about 0.37 eV and the $j_{H_2} = 1, j_{OH}=3$ peak occurs at lower energy around 0.363 eV.

These results should provide a starting point for comparison of theory and experiment and a test of the neutral potential energy surface. More *ab initio* calculations are needed to better define the anion potential before detailed comparisons can be made, however the prominent features seen in Figs. 4 and 5 should be a distinctive signature of the Anion I geometry.

V. CONCLUDING REMARKS

We have used the DVR-ABC method for reactive scattering to calculate initial state-selected reaction probabilities for the $OH+H_2$ reaction. We have demonstrated that this is an efficient method for such a large, multidimensional system. We believe that to treat reactions in large systems (four atoms and more) in an accurate way the logical approach will be to treat only a few degrees of freedom using rigorous quantum mechanical methods and incorporate the rest in some approximate (but accurate!) way. In that context, this reaction provides an excellent opportunity to test such reduced dimensionality methods on a large system for which full dimensional results are available. Many such methods have already been applied to reaction (1.1) and its reverse. We have shown that all the qualitative features—including resonance features—of the full dimensional calculations are obtained while freezing the OH bond and torsional angle. Clearly, this result will not apply for most reactions and the next step should be to test these methods on a variety of systems to determine their generality.

We have shown how the DVR-ABC formalism for generating the Green's function can be used to obtain total and arrangement-selected photodetachment intensities. We have used this method to calculate photodetachment spectra for *para* and *ortho* HOH_2^- and we are able to assign the features in the spectra according to a simple zeroth order model. These results provide an opportunity for comparison with experiment which will be a test of the accuracy of the neutral potential energy surface. However, due to its complicated nature more *ab initio* results are needed for the anion surface before a complete study can be undertaken.

ACKNOWLEDGMENTS

We wish to thank Professor Daniel M. Neumark for helpful comments on the photodetachment results. We also acknowledge Dr. Scott M. Auerbach for many useful discussions and for providing the Newton code and Dr. Tamar Seideman and Dr. Gerrit C. Groenenboom for the complex GMRES code. This work was supported by the Director, Office of Energy Research, Office of Basic Energy Sciences, Chemical Sciences Division of the U.S. Department of Energy under Contract No. DE-AC03-76SF00098. W.H.T. acknowledges support from the National Science Foundation.

[1] W. H. Miller, Ann. Rev. Phys. Chem. **41**, 245 (1990); D. E. Manolopoulos and D. C. Clary, Annu. Rep. C R. Soc. Chem. **86**, 95 (1989); M. D'Mello, D. E. Manolopoulos, and R. E. Wyatt, J. Chem. Phys. **94**, 5985 (1991); Chem. Phys. Lett. **168**, 113 (1990); J. D. Kress, R. B. Walker, and E. F. Hayes, J. Chem. Phys. **93**, 8085 (1990); J. D. Kress, R. B. Walker, E. F. Hayes, and P. Pendergast, *ibid.* **100**, 2728 (1994); I. Last, A. Baram, H. Szichman, and M. Baer, J. Phys. Chem. **97**, 7040 (1993); M. Gilibert, I. Last, A. Baram, and M. Baer, Chem. Phys. Lett. **221**, 327 (1994); T. J. Park and J. C. Light, J. Chem. Phys. **94**, 2946 (1991); T. J. Park and J. C. Light, *ibid.* **96**, 8853 (1992).

[2] D. C. Clary, J. Chem. Phys. **95**, 7298 (1991).

[3] D. C. Clary, J. Chem. Phys. **96**, 3656 (1992); Chem. Phys. Lett. **192**, 34 (1992).

[4] G. Nyman and D. C. Clary, J. Chem. Phys. **99**, 7774 (1993).

[5] J. Echave and D. C. Clary, J. Chem. Phys. **100**, 402 (1994).

[6] J. M. Bowman and D. Wang, J. Chem. Phys. **96**, 7852 (1992); D. Wang and J. M. Bowman, *ibid.* **96**, 8906 (1992); **98**, 6235 (1992).

[7] H. Szichman, I. Last, A. Baram, and M. Baer, J. Phys. Chem. **97**, 6436 (1993); **98**, 828 (1994).

[8] D. Zhang and J. Z. H. Zhang, J. Chem. Phys. **100**, 2697 (1994).

[9] D. Zhang and J. Z. H. Zhang, J. Chem. Phys. **101**, 1146 (1994).

[10] D. Neuhauser, J. Chem. Phys. **100**, 9272 (1994).

[11] U. Manthe, T. Seideman, and W. H. Miller, J. Chem. Phys. **99**, 10 078 (1994).

[12] S. P. Walch and T. H. Dunning, Jr., J. Chem. Phys. **72**, 1303 (1980).

[13] G. Wahnström, B. Carmeli, and H. Metiu, J. Chem. Phys. **88**, 2478 (1988).

[14] A. Garcia-vela, R. B. Gerber, and D. G. Imre, J. Chem. Phys. **97**, 7242 (1992).

[15] S. Keshavamurthy and W. H. Miller, Chem. Phys. Lett. **218**, 189 (1994).

[16] A. Sinha, M. C. Hsiao, and F. F. Crim, J. Chem. Phys. **92**, 6333 (1990); A. Sinha, M. C. Hsiao, and F. F. Crim, *ibid.* **94**, 4928 (1991).

[17] M. J. Bronikowski, W. R. Simpson, B. Girard, and R. N. Zare, J. Chem. Phys. **95**, 8647 (1991); J. Phys. Chem. **97**, 2194 (1993); **97**, 2204 (1993); D. E. Adelman, S. V. Filseth, and R. N. Zare, J. Chem. Phys. **98**, 4636 (1993).

[18] W. H. Miller and J. Z. H. Zhang, J. Phys. Chem. **95**, 12 (1991).

[19] D. M. Neumark, Acc. Chem. Res. **26**, 33 (1993); R. B. Metz, S. E. Bradforth, and D. M. Neumark, Adv. Chem. Phys. **81**, 1 (1992).

[20] A. Weaver, R. B. Metz, S. E. Bradforth, and D. M. Neumark, J. Chem. Phys. **93**, 5352 (1990); A. Weaver and D. M. Neumark, Faraday Discuss. Chem. Soc. **91**, 5 (1991); J. Z. H. Zhang, W. H. Miller, A. Weaver, and D. M. Neumark, Chem. Phys. Lett. **182**, 283 (1991); S. E. Bradforth, D. W. Arnold, and D. M. Neumark, J. Chem. Phys. **99**, 6345 (1993); D. E. Manolopoulos, K. Stark, H.-J. Werner, D. W. Arnold, S. E. Bradforth, and D. M. Neumark, Science (to be published).

[21] J. Z. H. Zhang and W. H. Miller, J. Chem. Phys. **92**, 1811 (1990).

[22] T. Seideman and W. H. Miller, J. Chem. Phys. **96**, 4412 (1992); **97**, 2499 (1992); W. H. Miller and T. Seideman, in *Time Dependent Quantum Molecular Dynamics: Experiment and Theory*, edited by J. Broeckhove (NATO ARW, 1992).

[23] W. H. Thompson and W. H. Miller, Chem. Phys. Lett. **206**, 123 (1993).

[24] S. M. Auerbach and W. H. Miller, J. Chem. Phys. **100**, 1103 (1994).

[25] D. O. Harris, G. G. Engerholm, and W. D. Gwinn, J. Chem. Phys. **43**, 1515 (1965).

[26] A. S. Dickinson and P. R. Certain, J. Chem. Phys. **49**, 4209 (1963).

[27] R. Meyer, J. Chem. Phys. **52**, 2053 (1970).

[28] C. C. Marston and G. G. Balint-Kurti, J. Chem. Phys. **91**, 3571 (1989).

[29] J. T. Muckerman, Chem. Phys. Lett. **173**, 200 (1990).
[30] C. Leforestier, J. Chem. Phys. **94**, 6388 (1991); J. A. Bentley, R. E. Wyatt, M. Menou, and C. Leforestier, *ibid.* **97**, 4255 (1992).
[31] R. A. Friesner, Chem. Phys. Lett. **116**, 39 (1985); J. Chem. Phys. **85**, 1462 (1986); **86**, 3522 (1987).
[32] R. Kosloff, NATO ASI Ser. C **412**, 175 (1993).
[33] W. Yang and A. C. Peet, Chem. Phys. Lett. **153**, 98 (1988); A. C. Peet and W. Yang, J. Chem. Phys. **90**, 1746 (1989).
[34] J. Echave and D. C. Clary, Chem. Phys. Lett. **190**, 225 (1992).
[35] D. T. Colbert and W. H. Miller, J. Chem. Phys. **96**, 1982 (1992).
[36] J. V. Lill, G. A. Parker, and J. C. Light, Chem. Phys. Lett. **89**, 483 (1982); J. C. Light, I. P. Hamilton, and J. V. Lill, J. Chem. Phys. **82**, 1400 (1985); Z. Bačić and J. C. Light, *ibid.* **85**, 4594 (1986); R. M. Whitnell and J. C. Light, *ibid.* **89**, 3674 (1988); S. E. Choi and J. C. Light, *ibid.* **92**, 2129 (1990).
[37] A. Goldberg and B. W. Shore, J. Phys. B **11**, 3339 (1978).
[38] C. Leforestier and R. E. Wyatt, J. Chem. Phys. **78**, 2334 (1983).
[39] R. Kosloff and D. Kosloff, J. Comput. Phys. **63**, 363 (1986).
[40] D. Neuhauser and M. Baer, J. Chem. Phys. **90**, 4351 (1989); D. Neuhauser and M. Baer, *ibid.* **91**, 4651 (1989); D. Neuhauser, M. Baer, and D. J. Kouri, *ibid.* **93**, 2499 (1990).
[41] G. Jolicard and E. J. Austin, Chem. Phys. Lett. **121**, 106 (1985); G. Jolicard and E. J. Austin, Chem. Phys. **103**, 295 (1986); G. Jolicard and M. Y. Perrin, *ibid.* **116**, 1 (1987); G. Jolicard, C. Leforestier, and E. J. Austin, J. Chem. Phys. **88**, 1026 (1988).
[42] I. Last, D. Neuhauser, and M. Baer, J. Chem. Phys. **96**, 2017 (1992); I. Last and M. Baer, Chem. Phys. Lett. **189**, 84 (1992); I. Last, A. Baram, and M. Baer, *ibid.* **195**, 435 (1992); I. Last, A. Baram, H. Szichman, and M. Baer, J. Phys. Chem. **97**, 7040 (1993).
[43] D. Wang and J. M. Bowman, J. Chem. Phys. **100**, 1021 (1994); R. C. Mayrhofer and J. M. Bowman, *ibid.* **100**, 7229 (1994).
[44] G. C. Schatz, J. Phys. Chem. **94**, 6157 (1990); G. C. Schatz, J. Chem. Phys. **90**, 3582 (1990); **90**, 4847 (1990); G. C. Schatz, D. Sokolovski, and J. N. L. Connor, *ibid.* **94**, 4311 (1991).
[45] G. C. Schatz and H. Elgersma, Chem. Phys. Lett. **73**, 21 (1980).
[46] S. M. Auerbach and C. Leforestier, Comput. Phys. Commun. **78**, 55 (1993).
[47] Y. Saad and M. H. Schultz, SIAM J. Sci. Stat. Comput. **7**, 856 (1986).
[48] M. H. Mok and J. C. Polanyi, J. Chem. Phys. **53**, 4588 (1970); B. A. Hodgson and J. C. Polanyi, *ibid.* **55**, 4745 (1971).
[49] G. C. Light and J. H. Matsumoto, Chem. Phys. Lett. **58**, 578 (1978).
[50] R. Zellner and W. Steinert, Chem. Phys. Lett. **81**, 568 (1981).
[51] G. P. Glass and B. K. Chaturvedi, J. Chem. Phys. **75**, 2749 (1981).
[52] M. Alagia, N. Balucani, P. Casavecchia, D. Stranges, and G. G. Volpi, J. Chem. Phys. **98**, 2459 (1993).
[53] S. S. Xantheas and T. H. Dunning, Jr. (preprint).